A Comparison of Two Rarefaction Models in the Compressible Reynolds Equation used in air bearing design for hard disk drives

Du Chen and David B. Bogy

Computer Mechanics Laboratory
Dept. of Mechanical Engineering
University of California
Berkeley, CA 94720

Abstract

Using the Kinetic theory approach, Kang [1] derived a molecular gas lubrication equation, which considered rarefaction effects in the presence of the asymmetric boundary conditions at the slider and disk surfaces. Also he established new databases of the flow rates for different surface accommodation coefficients. He suggested that the Fukui and Kaneko [2, 3] database (F-K model), which is often used in air bearing design codes, was incomplete and incorrect. Kang also analyzed the shear stresses due to the gaseous rarefaction and obtained databases of the shear stress coefficients for different surface accommodation coefficients. Here we implement Kang's results in the CML air bearing code and compare some static simulation results of the new simulator based on Kang's model with those of the former simulator based on the F-K model.

In the CML code the shear stress is calculated using the velocity profile of the first-order slip model [4] because of difficulties in calculating this quantity with the F-K model. In re-deriving this shear stress expression implemented in the CML code a sign error was discovered in the expressions used there. Here we correct the sign error and evaluate its effect on the simulation for a typical air bearing surface design. The effect is found to be of minor significance.

1. Introduction

The slider-disk separation in current hard disk drives (HDD) has become only a small fraction of the mean free path of the air. Therefore, the rarefaction effect of the gas layer has to be taken into account. Various slip correction models have been proposed by Burgdorfer [4] (first order slip), Hsia and Domoto [5] (second order slip) and Gans [6] (higher order slip). Fukui and Kaneko [2] derived a molecular gas lubrication model (F-K model) based on the linearized Boltzmann equation. It can also be cast in a form similar to the Reynolds equation with a flow rate coefficient. Fukui and Kaneko [3] also gave databases of the flow rate for symmetric accommodation coefficients of the slider and disk surfaces. The CML air bearing code has been using the results of the F-K model. But Fukui and Kaneko did not address the effect of air shear in their model.

When the slider and the disk are in the near contact region the effect of the shear force generated by the airflow under the air bearing may also be significant. And the shear force increases with the rotation speed of the disk. As observed by Lu [7], the omission of the shear force in the simulation may lead to an over-prediction of the slider's pitch. He used the velocity profile of the first-order slip model and then calculated the shear stress from the velocity gradient at the air-bearing surface. This method avoids the numerical difficulties of using the Boltzmann equation model of Fukui and Kaneko. And using it should not cause significant errors since the total shear force is small compared to the air bearing force, and also the first-order slip model solution is quite close to that of the F-K model. The current CML air bearing code uses this method to calculate the shear stress. However, the original derivation of the analytical expression for the shear force appears to have a sign error, which produced a corresponding error in the code.

To consider the effect of air rarefaction and air shear Kang [1] used a different approach in his dissertation. Using kinetic theory Kang derived a molecular gas lubrication equation, which considered the change of the rarefaction due to the asymmetric boundary conditions at the slider and disk surfaces, and he also obtained new databases for the flow rates for different surface accommodation coefficients. He stated that the Fukui and Kaneko database, which is used by the CML code, was incomplete and incorrect. Kang also analyzed the shear stresses due to the gaseous rarefaction and

obtained the databases of the shear stress coefficients for different surface accommodation coefficients. The comparison of the static simulation results using a new simulator based on Kang's model with those of the former simulator, both the original and corrected versions, shows little difference in the flying altitude of flying sliders. The maximum difference in the minimum flying height is less than 2% for commonly used surface accommodation coefficients of about 0.95.

2. The Shear Stress Formula Based on the First Order Slip Model

The first order slip model uses the wall slip boundary conditions to incorporate the gas rarefaction into the lubrication theory. The slip velocity is a function of the slip distance ζ_{slip} and the velocity gradients obtained at the boundaries $\partial u/\partial n\big|_{wall}$. Based on Maxwell's formula for ζ_{slip},

$$u_{slip} = \zeta_{slip} \left.\frac{\partial u}{\partial n}\right|_{wall} = a\lambda \left.\frac{\partial u}{\partial n}\right|_{wall},$$

where $a = \dfrac{2-\alpha}{\alpha}$, α is the surface accommodation coefficient, a is called the surface accommodation factor and λ is the local molecular mean free path.

The non-dimensionalized reduced Navier-stokes equations for the gas film are,

$$\begin{aligned} -\frac{6}{\Lambda_x}\frac{\partial P}{\partial X} + \frac{\partial^2 U}{\partial Z^2} &= 0, \\ -\frac{6}{\Lambda_y}\frac{\partial P}{\partial Y} + \frac{\partial^2 V}{\partial Z^2} &= 0, \\ \frac{\partial P}{\partial Z} &= 0, \end{aligned} \tag{1}$$

where $P = p/p_a, X = x/L, Y = y/L, H = h/h_m, U = u/U^*, V = v/V^*$ are the non-dimensional pressure, coordinate in the slider's length direction, coordinate in the slider's width direction, bearing clearance and air velocity components in the *x* and *y* directions, respectively; p_a is the ambient atmospheric pressure; h_m is the reference clearance at the trailing edge center; L is the length of the slider; $\Lambda_x = \dfrac{6\mu U^* L}{p_a h_m^2}$ and $\Lambda_y = \dfrac{6\mu V^* L}{p_a h_m^2}$ are the

bearing numbers in the *x* and *y* directions, respectively; U^* and V^* are the disk *x* and *y* velocity components, respectively.

The boundary conditions for the first order slip flow can be expressed as:

$$u = U^* + u_{slip} = U^* + a\lambda \frac{\partial u}{\partial z},\ v = V^* + v_{slip} = V^* + a\lambda \frac{\partial v}{\partial z}, \text{ at } z = 0;$$
$$u = u_{slip} = -a\lambda \frac{\partial u}{\partial z},\ v = v_{slip} = -a\lambda \frac{\partial v}{\partial z}, \text{ at } z = h.$$

The corresponding non-dimensional boundary conditions are:

$$\begin{aligned} U &= 1 + aK_n \frac{\partial U}{\partial Z}, V = 1 + aK_n \frac{\partial V}{\partial Z}, \text{ at Z=0;} \\ U &= -aK_n \frac{\partial U}{\partial Z}, V = -aK_n \frac{\partial V}{\partial Z}, \text{ at Z=H.} \end{aligned} \tag{2}$$

where $K_n = \frac{\lambda}{h_m}$ is the Knudsen number and λ is the mean free path of the air.

Solving equations (1) and (2) we can obtain a velocity profile with first order slip,

$$\begin{aligned} U &= \frac{3}{\Lambda_x}\frac{dP}{dX}[Z^2 - (Z + aK_n)H] + 1 - \frac{Z + aK_n}{2aK_n + H} \\ V &= \frac{3}{\Lambda_y}\frac{dP}{dY}[Z^2 - (Z + aK_n)H] + 1 - \frac{Z + aK_n}{2aK_n + H} \end{aligned} \tag{3}$$

The shear stress components in the air acting at the air-bearing surface are,

$$\tau_x = -\mu \left.\frac{\partial u}{\partial z}\right|_{z=h} \text{ and } \tau_y = -\mu \left.\frac{\partial v}{\partial z}\right|_{z=h}.$$

With the velocity profile equation (3) the shear stress non-dimensionalized by $p_a h_m / L$ is,

$$\mathrm{T}_x = -\frac{H}{2}\frac{\partial P}{\partial X} + \frac{\Lambda_x}{6(2aK_n + H)}$$
$$\mathrm{T}_y = -\frac{H}{2}\frac{\partial P}{\partial Y} + \frac{\Lambda_y}{6(2aK_n + H)}$$

So the pitch and roll moments of the total shear force acting on the slider with respect to the suspension load point, non-dimensionalized by $p_a L^3$, can be expressed as:

$$S_x = c(\frac{h_m}{L})\int_0^b \int_0^1 [-\frac{H}{2}\frac{\partial P}{\partial X} + \frac{\Lambda_x}{6(2aK_n + H)}]dXdY$$
$$S_y = c(\frac{h_m}{L})\int_0^b \int_0^1 [-\frac{H}{2}\frac{\partial P}{\partial Y} + \frac{\Lambda_y}{6(2aK_n + H)}]dXdY \quad (4)$$

where c and b are the slider thickness and width non-dimensionalized by L, respectively.

Lu's [7] expression for S_x and S_y are

$$S_x = c(\frac{h_m}{L})\int_0^b \int_0^1 [\frac{H}{2}\frac{\partial P}{\partial X} + \frac{\Lambda_x}{6(H + 2K_n)}]dXdY$$
$$S_y = c(\frac{h_m}{L})\int_0^b \int_0^1 [\frac{H}{2}\frac{\partial P}{\partial Y} + \frac{\Lambda_y}{6(H + 2K_n)}]dXdY$$

Therefore Lu's results have the opposite sign for the $\frac{\partial P}{\partial X}$ and $\frac{\partial P}{\partial Y}$ terms and consider only the case $a = 1$, i.e. the surface accommodation coefficient is 1.

The current CML code uses Lu's results to calculate the pitch and roll moments of the air shear. This overestimates the shear stress.

3. Kang's databases

Fukui and Kaneko [2] derived a generalized lubrication equation based on the Boltzmann equation, which can be cast in a form similar to the Reynolds equation incorporating the Poiseuille flow rate Q_p. It can be written as the following non-dimensional steady state generalized Reynolds Equation,

$$\frac{\partial}{\partial X}(\frac{Q_p}{D/6}PH^3\frac{\partial P}{\partial X}) + \frac{\partial}{\partial Y}(\frac{Q_p}{D/6}PH^3\frac{\partial P}{\partial Y}) = \Lambda_x\frac{\partial (PH)}{\partial X} + \Lambda_y\frac{\partial (PH)}{\partial Y}. \quad (5)$$

Also Fukui and Kaneko [3] published a database of Q_p for high Knudsen numbers and various surface accommodation coefficients of the slider and the disk ($\alpha_{slider} = \alpha_{disk}$). The current CML Air program uses this database.

Later Kang [1] derived, from the Bhatnagar-Gross-Krook (BGK) kinetic equation, a generalized Reynolds equation that incorporates both the Poiseuille flow rate Q_p and the Couette flow rate Q_c,

$$\frac{\partial}{\partial x}(\frac{6}{D}ph^3Q_p\frac{\partial p}{\partial x})+\frac{\partial}{\partial x}(\frac{6}{D}ph^3Q_p\frac{\partial p}{\partial y})=6\mu U^*\frac{\partial(Q_c ph)}{\partial x}+6\mu V^*\frac{\partial(Q_c ph)}{\partial y}+12\mu\frac{\partial(ph)}{\partial t},$$

where p is the air bearing pressure, μ is the viscosity of the air and U* and V* are the disk velocity components in the x and y directions, respectively. The corresponding non-dimensional static equation is,

$$\frac{\partial}{\partial X}(\frac{Q_p}{D/6}PH^3\frac{\partial P}{\partial X})+\frac{\partial}{\partial Y}(\frac{Q_p}{D/6}PH^3\frac{\partial P}{\partial Y})=\Lambda_x\frac{\partial(Q_c PH)}{\partial X}+\Lambda_y\frac{\partial(Q_c PH)}{\partial Y}. \qquad (6)$$

In addition, in Kang's treatment the gaseous rarefaction influences the wall shear stresses (τ_x and τ_y) exerted on the air-bearing surface, which can be explicitly expressed as Couette and Poiseuille flow contributions by

$$\tau_x=-\frac{h}{2}\frac{\partial p}{\partial x}w_p+\frac{\mu U^*}{h}w_c,$$
$$\tau_y=-\frac{h}{2}\frac{\partial p}{\partial y}w_p+\frac{\mu V^*}{h}w_c.$$

The shear stress components non-dimensionalized by $p_a h_m / L$ are,

$$\mathrm{T}_x=-\frac{H}{2}\frac{\partial P}{\partial X}w_p+\frac{\Lambda_x}{6H}w_c,$$
$$\mathrm{T}_y=-\frac{H}{2}\frac{\partial P}{\partial Y}w_p+\frac{\Lambda_y}{6H}w_c.$$

A numerical analysis using the Boltzmann equation with the above BGK model was performed to calculate Q_p, Q_c, w_p and w_c. Databases of these quantities for selected surface accommodation coefficients (α_{slider}, α_{disk}) are given in Kang's dissertation [1].

When $\alpha_{slider}=\alpha_{disk}$, $Q_c=1$. Then (6) reduces to (5). But Kang's databases of Q_p still differ from those of F-K, which, according to Kang, " fails to give correct asymptotic behavior at high D".

4 Implementation of Kang's databases into the CML code

Kang's model considers the effect of air rarefaction and air shear on the air bearing. In this section we implement Kang's model in the CML code and use Kang's databases for flow rate Q_p and shear coefficient w_p and w_c.

When we implemented the F-K model in the code using the F-K database we obtained power series expressions for numerically calculated flow rate coefficients Q_p in each of the three regions of the scattered inverse Knudsen number D [3]. The code uses these power series expressions to calculate Q_p for different D.

For convenience we presently just use spline interpolation to obtain a certain Q_p, w_p and w_c for different D from Kang's databases with $0.01 \le D \le 100$. When D is not in the region of the table, we calculate Q_p, w_p and w_c from

if $D<0.01$, $Q_p = -\dfrac{\log_{10} D}{\sqrt{\pi}}$, i.e., the limit of Q_p;

$$w_p = 1, w_q = 0,$$

if D>100,

$$Q_p = 0.1681D + 1.4 + 1.98/D - 5.181/D^2 \quad \text{for } \alpha = 0.80,$$
$$Q_p = 0.1667D + 1.229 + 0.886/D - 1.242/D^2 \quad \text{for } \alpha = 0.90,$$
$$Q_p = 0.1667D + 1.118 + 0.937/D - 1.346/D^2 \quad \text{for } \alpha = 0.95,$$
$$Q_p = 0.1666D + 1.023 + 0.8899/D - 1.151/D^2 \quad \text{for } \alpha = 1.00,$$

i.e., the power series of Q_p in terms of D based on the database in the region $5 < D < 100$;

$$w_p = 1, w_q = 1,$$ i.e., the continuous case.

5. Simulation Results

(1) Flow rate databases of the F-K model and Kang's model

The F-K model only addresses the case of symmetric surface accommodation coefficients, i.e., $\alpha_{slider} = \alpha_{disk}$. For that case, the only difference between the F-K model and Kang's model is in the Poiseuille flow rate, since Kang's model gives the Couette flow rate $Q_c = 1$ for $\alpha_{slider} = \alpha_{disk}$. Figure 1 shows the comparison between these two models' databases for the Poiseuille flow rate Q_p with $\alpha_{slider} = \alpha_{disk} = 0.80,\ 0.90, 0.95, 1.00$. We see that the maximum difference between them is less than 10%, which occurs when $\alpha_{slider} = \alpha_{disk} = 0.80$. There is no difference at $\alpha_{slider} = \alpha_{disk} = 1.00$.

(2) Femto Slider

Figure 2 shows a negative pressure Femto slider design for a 0.8g suspension force and zero moment suspension pre-load and a disk rotation speed of 5000 rpm. The skew angle is zero. Table 1 shows the simulation results with Kang's model (Simulator 1), which includes the shear stress calculation based on the Kang's shear stress coefficient databases. It also shows results based on the F-K model, which includes the old shear stress calculation based on Lu's dissertation (Simulator 3) and the corrected shear stress calculation of equation 4 (Simulator 2). To avoid the additional influence of non-linear intermolecular force, we do not consider surface adhesion in the simulation. Table 1 shows that the results obtained from these three simulators are quite close to each other. Due to zero skew angle, the shear force in the y direction, i.e., slider width direction, is close to zero. And the shear forces in the x direction obtained from Simulator 1 and Simulator 2 are much closer than those from Simulator 1 and Simulator 3. The main reason is that Lu's expressions for shear stress has the sign error. And also they consider only the case $\alpha_{slider} = \alpha_{disk} = 1.00$, which means that the shear stress calculation always assumes the surface accommodation coefficient is 1. Figure 3 shows the comparison between the simulation results obtained from Simulator 1 and Simulator 2. The maximum difference is less than 8% and it occurs when $\alpha_{slider} = \alpha_{disk} = 0.80$. This is reasonable since the databases of Kang's model and the F-K model are close, and the maximum difference occurs when $\alpha_{slider} = \alpha_{disk} = 0.80$. The shear forces obtained from Simulator 1 is close to that from Simulator 2. This verifies that the corrected shear stress calculation based on the velocity profile of the first-order slip does not produce a significant difference from Kang's model.

(3) Pico Slider

Figure 4 shows a Pico slider design for a 1.5g suspension force and zero moment suspension pre-load and a disk rotation speed of 10000 rpm. The skew angle is 8 degrees. The steady state flying height is around 10nm. Table 2 shows the simulation results for Simulator1, 2 and 3.. Intermolecular force is considered in the simulations, with Hamaker constants $A = 2.79 \times 10^{-19} J, B = 1 \times 10^{-76} Jm^6$. As with the Femto case the results obtained from these three simulators are quite close to each other. And both of the shear forces in x

direction and y direction obtained from Simulator 1 and Simulator 2 are much closer than those from Simulator 1 and Simulator 3. The reasons are the same, the sign error is corrected in Simulator 2. Figure 5 shows the comparison between the simulation results obtained from Simulator 1 and Simulator 2. The maximum difference in the flying height is less than 14% and it occurs when $\alpha_{slider} = \alpha_{disk} = 0.80$. But for $\alpha_{slider} = \alpha_{disk} = 0.90$, 0.95, 0.10, the difference in the flying height is less than 1%.

Conclusions

The analytical expressions for the shear stress are re-derived based on the velocity profile of the first-order slip model. It is found that Lu's [7] derivation contained a sign error. This error led to a corresponding error in the CML air bearing code. A modified simulator (Simulator 2) is obtained by correcting the error. Also Kang's model is implemented into the code and takes the place of the F-K databases and the shear stress calculation based on the first order slip model. A new simulator (Simulator 1) is obtained using Kang's model. For Pico and Femto sliders, the comparison of the static simulation results using Simulator 1 with those using Simulator 2 shows little difference in flying altitude of the flying sliders. The maximum difference in the minimum flying height is less than 2% for commonly used surface accommodation coefficients around 0.95. Also the shear forces obtained from Simulator 2 are quite close to those obtained from Simulator 1. So using the F-K model and shear stress calculation based on the first-order slip model does not cause a significant difference from using Kang's model in air bearing simulations when considering the air rarefaction and air shear.

References

[1] Soo-Choon Kang (1997), “A Kinetic Theory Description for Molecular Lubrication,” Dissertation

[2] Fukui, S. and Kaneko,R (1987), “Analysis of Ultra-Thin Gas Film Lubrication Based on Linearized Boltzmann Equation (Influence of Accommodation Coefficient),” JSME International Journal **30**, 1660-1666

[3] Fukui, S and Kaneko,R (1990), “ A Database for Interpolation of Poiseuille Flow Rates for Hight Knudsen Number Lubrication Problems,” ASME Journal of Tribology **112**, 78-83

[4] Burgdorfer, A. (1959), “The influence of the Molecular Mean Free Path on the performance of Hydrodynamic Gas Lubricated Beraings,” ASME Journal of Basic Engineering **81**, 94-100

[5] Hsia, Y.T. and Domoto, G.A. (1983), “An Experimental Investigation of Molecular Rarefaction Effects in Gas Lubricated Bearings at Ultra –Low Clearances,” ASME Journal of Lubrication Technology **105**, 120-130

[6] Gans, R. (1985), “Lubrication Theory at Arbitrary Knudsen Number,” ASME Journal of Tribology **107**, 431-433

[7] Sha Lu (1997), “Numerical Simulation of Slider Air Bearings,” Dissertation

Table 1. The Simulation Results for the Femto Slider
with $\alpha_{slider} = \alpha_{disk} = 0.80,\ 0.90, 0.95, 1.00$

$\alpha_{slider} = \alpha_{disk} = 1.00$

	FH (nm)	Pitch (μrad)	Roll (μrad)	X-Shear Force (g)	Y-Shear Force (g)
Kang Model (Simulator 1)	6.41072	117.214	-0.889475	0.022627	5E-006
F-K Model (Simulator 2)	6.43049	116.937	-0.947444	0.023894	8E-006
F-K Model (Simulator 3)	6.50821	116.217	-0.862061	0.034475	-2.5E-005

$\alpha_{slider} = \alpha_{disk} = 0.95$

	FH (nm)	Pitch (μrad)	Roll (μrad)	X-Shear Force (g)	Y-Shear Force (g)
Kang Model (Simulator 1)	6.0238	112.242	-0.834897	0.02131	1E-005
F-K Model (Simulator 2)	5.99141	114.784	-0.867624	0.022302	1.3E-005
F-K Model (Simulator 3)	6.06948	113.851	-0.879952	0.034657	-2.4E-005

$\alpha_{slider} = \alpha_{disk} = 0.90$

	FH (nm)	Pitch (μrad)	Roll (μrad)	X-Shear Force (g)	Y-Shear Force (g)
Kang Model (Simulator 1)	5.67634	107.178	-0.821837	0.020002	1.4E-005
F-K Model (Simulator 2)	5.59559	103.581	-0.736298	0.0212	1.8E-005
F-K Model (Simulator 3)	5.67696	102.666	-0.72976	0.035234	-2.1E-005

$\alpha_{slider} = \alpha_{disk} = 0.80$

	FH (nm)	Pitch (μrad)	Roll (μrad)	X-Shear Force (g)	Y-Shear Force (g)
Kang Model (Simulator 1)	5.06242	96.7775	-0.720392	0.017439	2E-005
F-K Model (Simulator 2)	4.66956	93.0974	-0.660202	0.018375	2.4E-005
F-K Model (Simulator 3)	5.15605	101.492	-0.730179	0.035399	-2.1E-005

Table 2. The Simulation Results for the Pico Slider
with $\alpha_{slider} = \alpha_{disk} = 0.80,\ 0.90, 0.95, 1.00$

$\alpha_{slider} = \alpha_{disk} = 1.00$

	FH (nm)	Pitch (μrad)	Roll (μrad)	X-Shear Force (g)	Y-Shear Force (g)
Kang Model (Simulator 1)	10.0719	277.894	-0.551928	0.07433	-0.010225
F-K Model (Simulator 2)	10.0964	277.751	-0.514417	0.078025	-0.010759
F-K Model (Simulator 3)	10.137	277.159	-0.252911	0.094362	-0.013856

$\alpha_{slider} = \alpha_{disk} = 0.95$

	FH (nm)	Pitch (μrad)	Roll (μrad)	X-Shear Force (g)	Y-Shear Force (g)
Kang Model (Simulator 1)	9.40008	271.062	-0.928997	0.071751	-0.009855
F-K Model (Simulator 2)	9.39180	274.671	-1.00267	0.074841	-0.010291
F-K Model (Simulator 3)	9,49117	273.942	-0.739974	0.094998	-0.013935

$\alpha_{slider} = \alpha_{disk} = 0.90$

	FH (nm)	Pitch (μrad)	Roll (μrad)	X-Shear Force (g)	Y-Shear Force (g)
Kang Model (Simulator 1)	8.71139	263.673	-1.33093	0.069166	-0.009487
F-K Model (Simulator 2)	8.69424	260.461	-1.17585	0.072843	-0.010027
F-K Model (Simulator 3)	8.72852	260.164	-1.13424	0.080648	-0.011185

$\alpha_{slider} = \alpha_{disk} = 0.80$

	FH (nm)	Pitch (μrad)	Roll (μrad)	X-Shear Force (g)	Y-Shear Force (g)
Kang Model (Simulator 1)	7.38851	247.470	-1.82536	0.063779	-0.008731
F-K Model (Simulator 2)	6.40846	244.555	-2.66303	0.067173	-0.009208
F-K Model (Simulator 3)	7.66661	256.706	-1.79933	0.097933	-0.014297

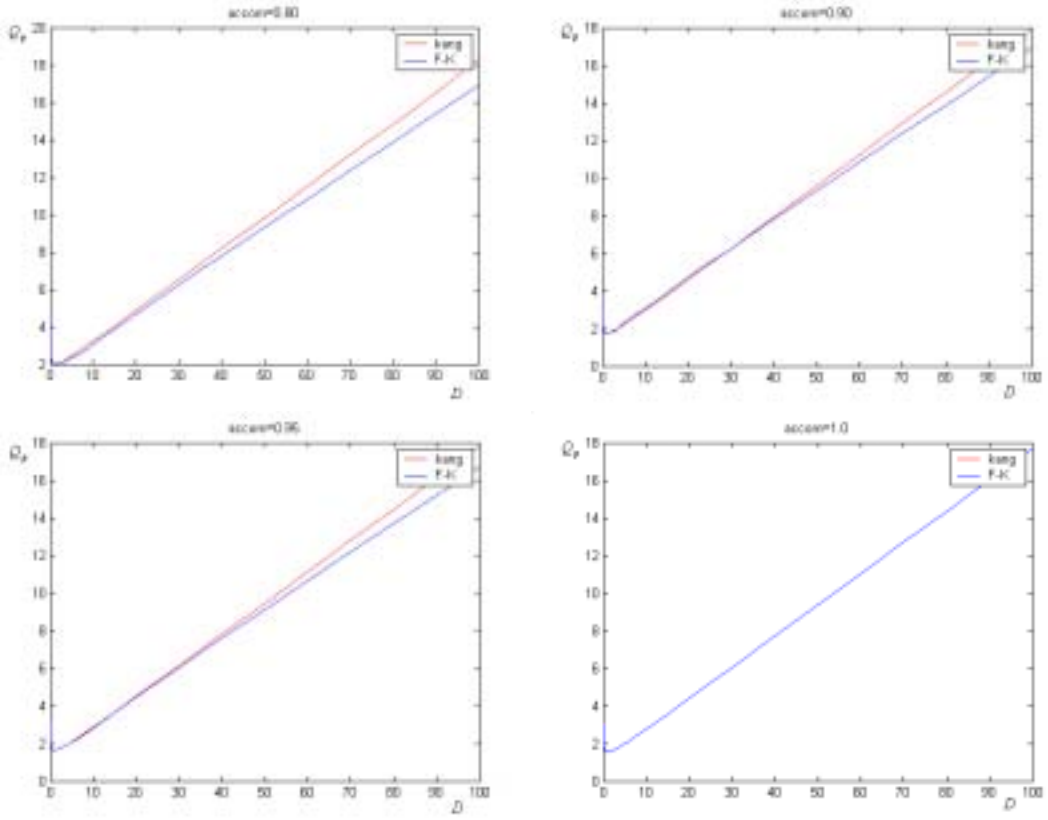

Fig. 1 The Poiseuille flow rate Q_p vs. inverse Knudsen Number D for $\alpha_{slider} = \alpha_{disk} = 0.80,\ 0.90,\ 0.95,\ 1.00$

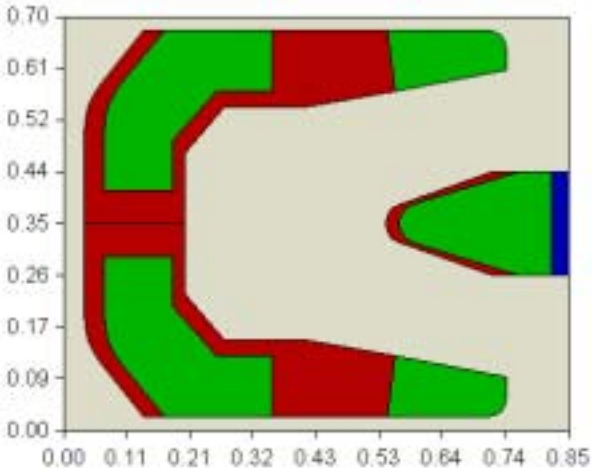

Fig. 2 the Femto Slider

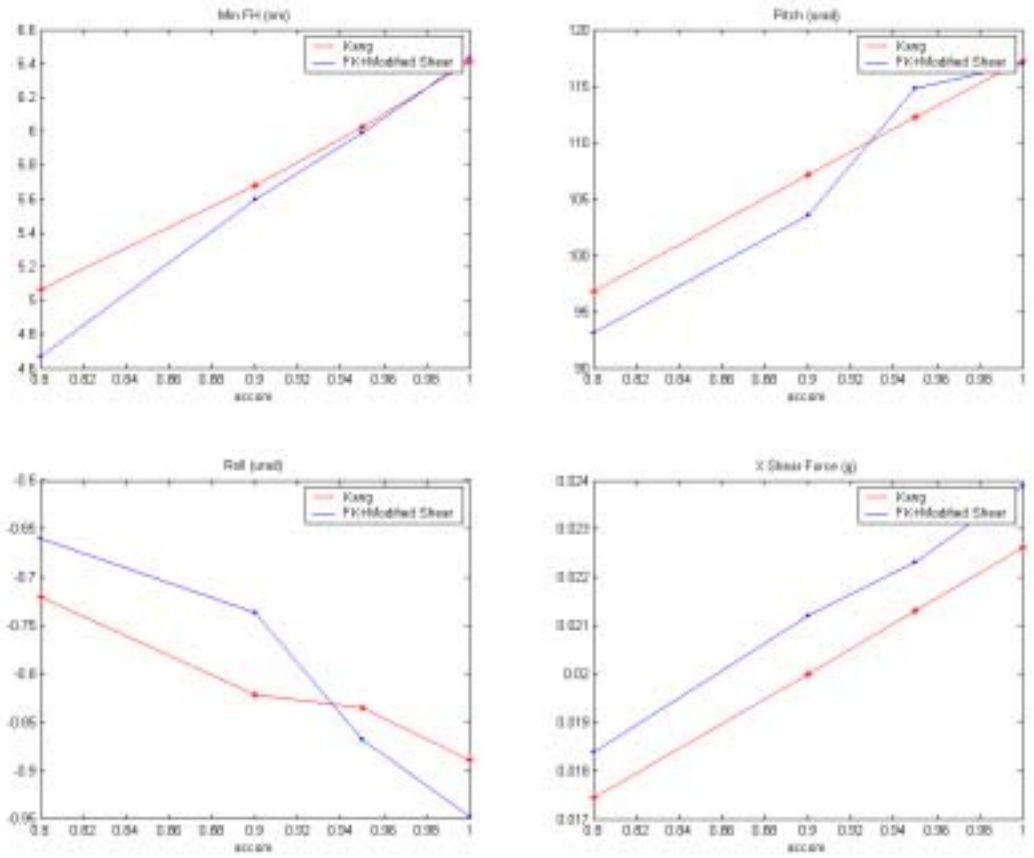

Fig. 3 the Comparison of the Simulation Results of the Femto Slider from Kang model (simulator 1) and F-K model (simulator 2)

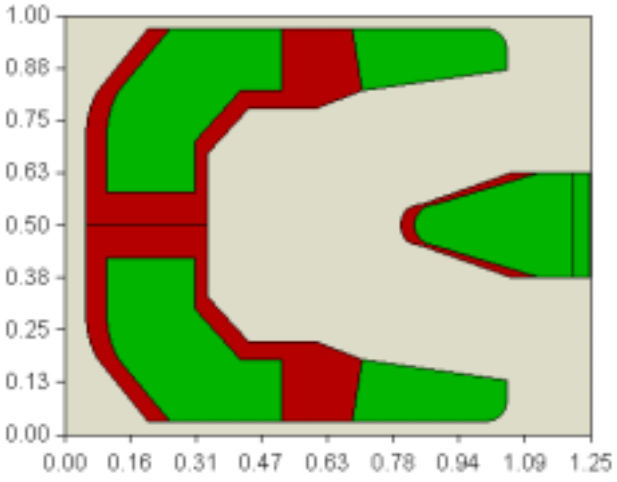

Fig. 4 the Pico slider

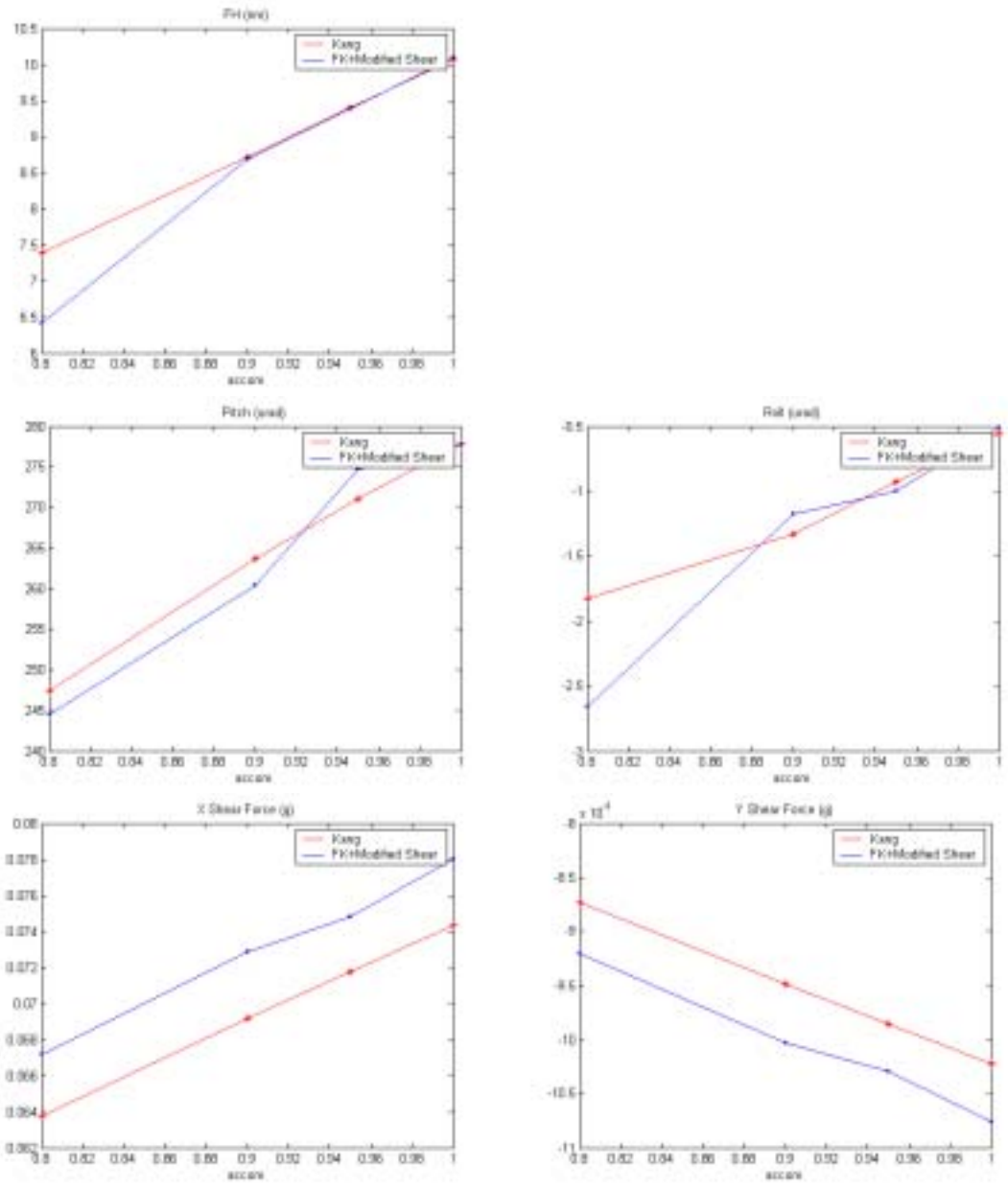

Fig. 5 the Comparison of the Simulation Results of the Pico Slider
from Kang model (simulator 1) and F-K model (simulator 2)